

Supplementary figure legends:

Figure S1: FACS sorting gating criteria

(A) FACS histograms showing the sorting gates for the CD44^v^{high} and CD44^v^{low} from the CD44v-expressing cell line, H1650. (B) FACS histograms showing the sorting gates for pan CD44^{high} and pan CD44^{low} from the CD44v-non-expressing cell line, A549. (C, D) FACS dot plots showing the sorting gates for CD44^v^{high}/ALDH^{high}, CD44^v^{high}/ALDH^{low}, CD44^v^{low}/ALDH^{high} and CD44^v^{low}/ALDH^{low} cells from H1650 and HCC827 cell lines.

Figure S2: Xenograft tumor formation

(A, B) 100,000 CD44^v^{high}/ALDH^{high}, CD44^v^{high}/ALDH^{low}, CD44^v^{low}/ALDH^{high}, CD44^v^{low}/ALDH^{low} cells were sorted from the CD44v-expressing cell lines, H1650 and HCC827, and transplanted into immunocompromised mice, H1650: n=9 and HCC287: n=9.

Figure S3: Comparison of the ability of different populations sorted from H1650 cells to form anchorage-independent colonies (tumorspheres)

The sorted four populations from H1650 cells were seeded in suspension in 1000, 500, 100, 50, 10 and 1 cell/well and observed for the presence of >200 µm tumorspheres for 2-4 weeks.

(A) A cartoon showing number of wells containing at least one tumorsphere from each cell type in relation to number of seeded cells. (B) Graph presentation of the relation between number of cells/well and percentage of wells with at least one tumorsphere in each cell type. (C) Representative colony images are shown.

Figure S4: Comparison of the ability of different populations sorted from HCC827 cells to form anchorage-independent colonies (tumorspheres)

The sorted four populations from HCC827 cells were seeded in suspension in 1000, 500, 100, 50, 10 and 1 cell/well and observed for the presence of >200 µm tumorspheres for 2-4 weeks.

(A) A cartoon showing number of wells containing at least one tumorsphere from each cell type in relation to number of seeded cells. (B) Graph presentation of the relation between number of cells/well and percentage of wells with at least one tumorsphere in each cell type. (C) Representative colony images.

Figure S5: FACS sorting using a strict gating criteria

(A, B) FACS dot plots showing the sorting gates for CD44^v^{high}/ALDH^{high}, CD44^v^{high}/ALDH^{low}, CD44^v^{low}/ALDH^{high} and CD44^v^{low}/ALDH^{low} cells from H1650 and HCC827 cell lines. The gates were set to sort less than 5% for each population.

Figure S6: Comparison of the ability of different populations strictly sorted from H1650 cells to form anchorage-independent colonies (tumorspheres)

The strictly sorted four populations from H1650 cells were seeded in suspension in 1000, 500, 100, 50, 10 and 1 cell/well and observed for the presence of >200 µm tumorspheres for 2-4 weeks.

(A) A cartoon showing number of wells containing at least one tumorsphere from each cell type in relation to number of seeded cells. (B) Graph presentation of the relation between number of cells/well and percentage of wells with at least one tumorsphere in each cell type. (C) Representative colony images.

Figure S7: Comparison of the ability of different populations strictly sorted from HCC827 cells to form anchorage-independent colonies (tumorspheres)

The strictly sorted four populations from HCC827 cells were seeded in suspension in 1000, 500, 100, 50, 10 and 1 cell/well and observed for the presence of >200 µm tumorspheres for 2-4 weeks.

(A) A cartoon showing number of wells containing at least one tumorsphere from each cell type in relation to number of seeded cells. (B) Graph presentation of the relation between number of cells/well and percentage of wells with at least one tumorsphere in each cell type. (C) Representative colony images.

Figure S8: Association between xenograft necrotic area size and genotypes of initiating cells from the H1650 cell line

Tumor blocks were sectioned half way through the longest axis to expose the widest surface area possible. Sections were stained with H&E and imaged. (A) Representative tumors from the four populations of the H1650 cell line. (B) The necrotic area/total tumor area % from at least 5 tumors were measured.

Figure S9: Association between xenograft necrotic area size and genotypes of initiating cells from the HCC827 cell line

Tumor blocks were sectioned half way through the longest axis to expose the widest surface area possible. Sections were stained with H&E and imaged. **(A)** Representative tumors from the four populations of the HCC827 cell line. **(B)** The necrotic area/total tumor area % from at least 5 tumors were measured.

Figure S10: Association between stroma amount and genotypes of initiating cells

Sections from xenografts from all the four populations, from both H1650 and HCC827 cell lines, were immunostained for e-cadherin and CD34, which mark cancer and stromal cells, respectively. Percentages of stromal to tumor area were measured. No significant differences were detected among the four populations from either cell line. **(A)** Representative image from a CD44^v^{high}/ALDH^{high} tumor from HCC827. **(B)** Representative high power image. Scale bars: A=200 μ m, B=50 μ m.

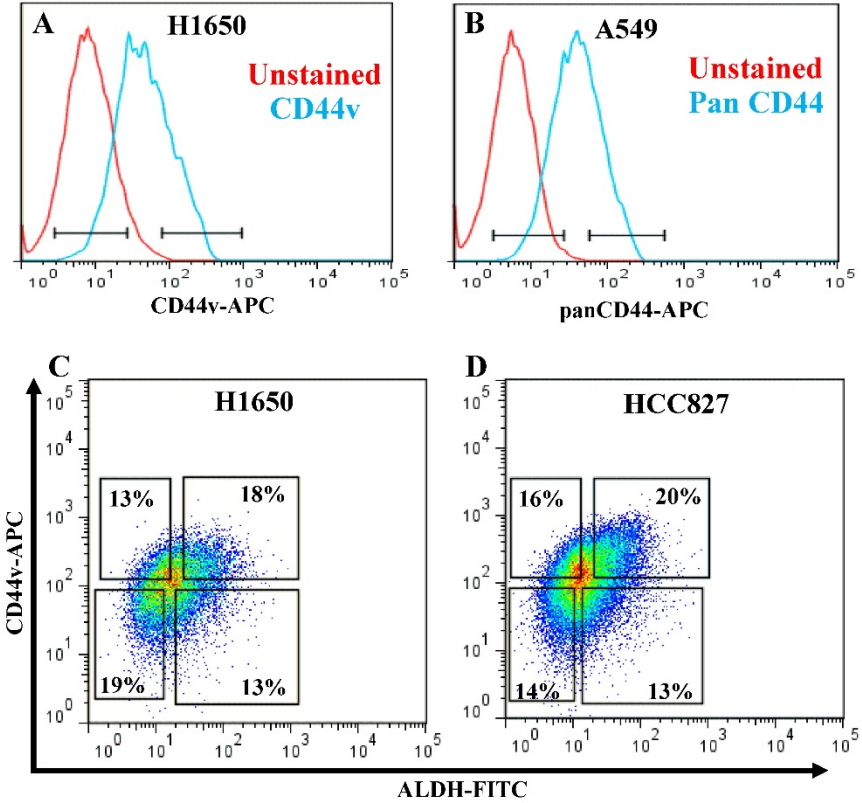
Figure S11: EGFR expression is not associated with CD44^v^{high} expression

Freshly sorted HCC827 cells were cytospun and immunostained for EGFR (red) and pEGFR (green). Representative images from H1650: **(A)** CD44^v^{high}/ALDH^{high}, **(B)** CD44^v^{high}/ALDH^{low}, **(C)** CD44^v^{low}/ALDH^{high} and **(D)** CD44^v^{low}/ALDH^{low} cells. Nuclei were stained with DAPI. Scale bars: 20 μ m. **(E)** shows quantification of fluorescence intensity. No significant differences were detected among the different populations.

Figure S12: Effect of differentiation expression of CD44v and ALDH on ROS level

Freshly sorted CD44^v^{high}/ALDH^{high}, CD44^v^{high}/ALDH^{low}, CD44^v^{low}/ALDH^{high} and CD44^v^{low}/ALDH^{low} cells from H1650 and HCC827 cell lines were stained with H2DCFDA and their ROS levels were compared by flow cytometry.

Figure S1



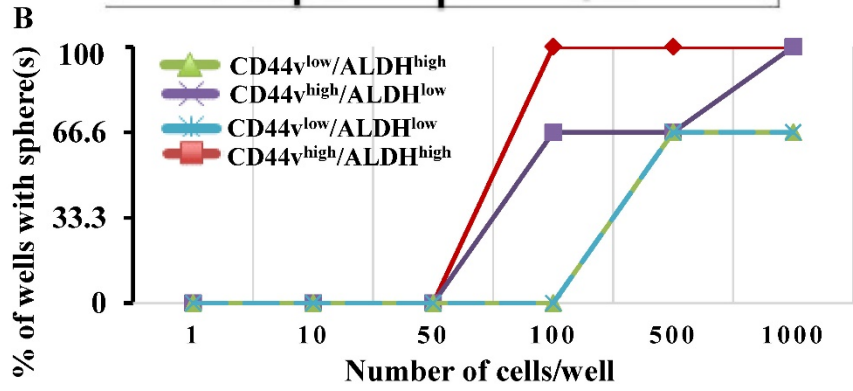
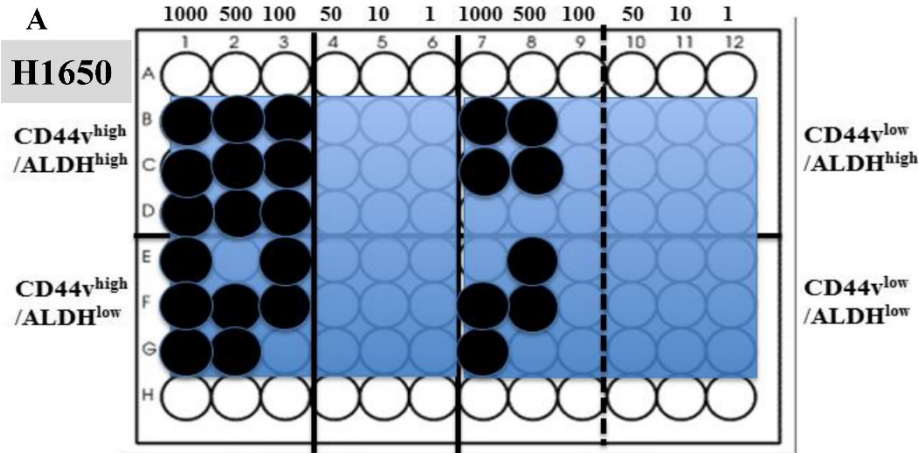
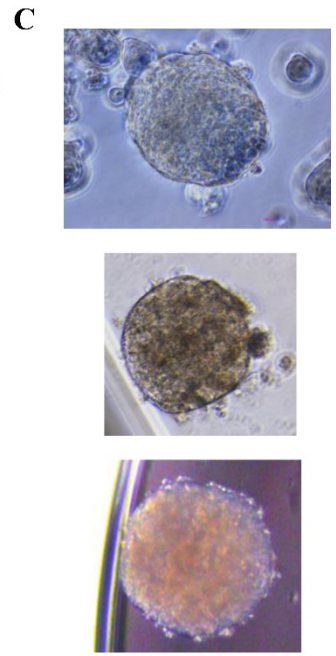


Figure S3



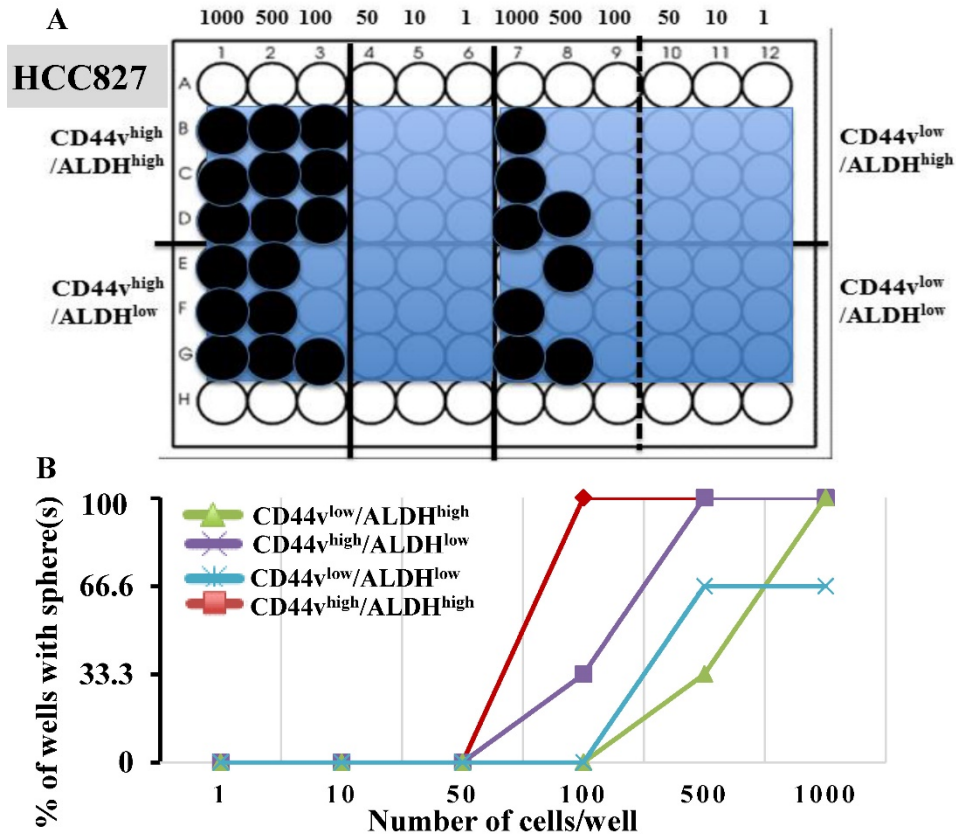
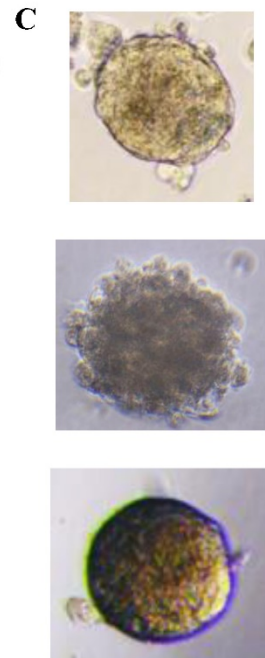


Figure S4



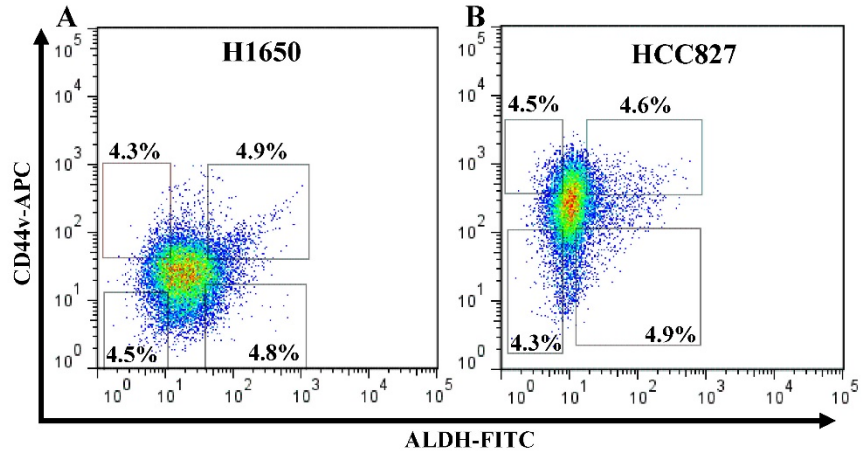


Figure S5

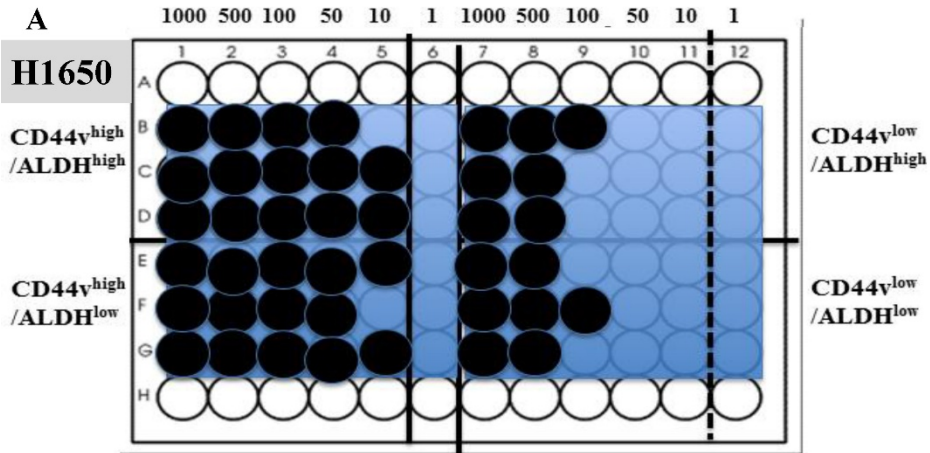
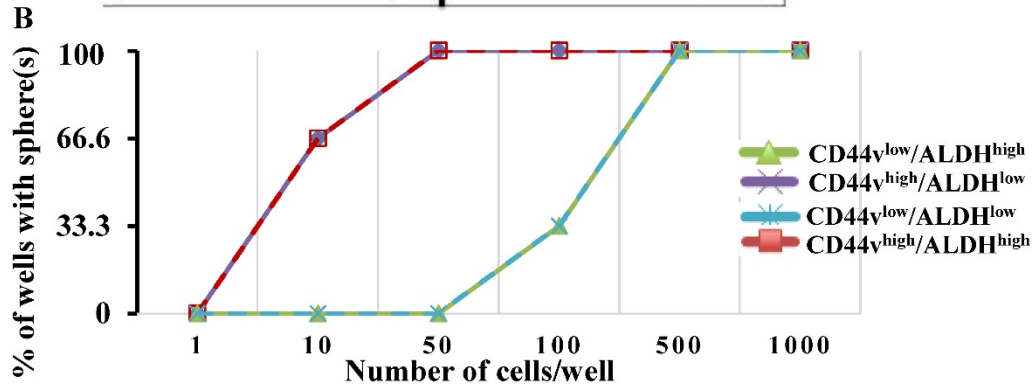


Figure S6



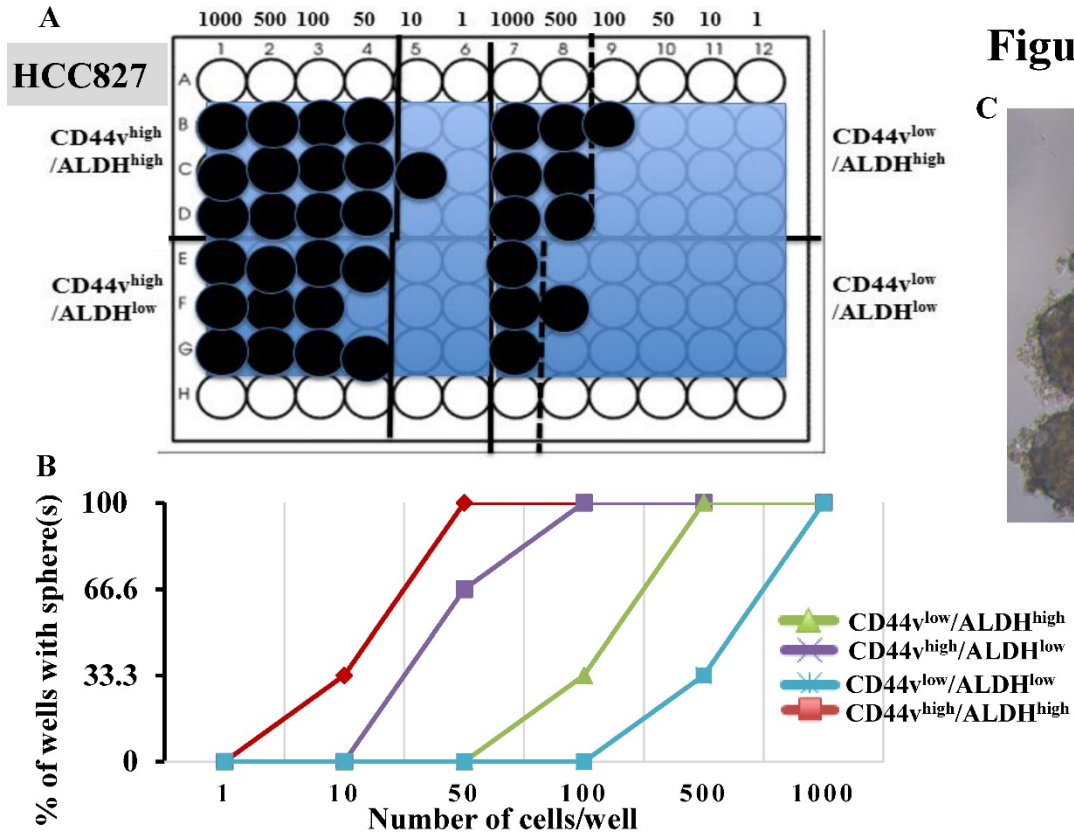
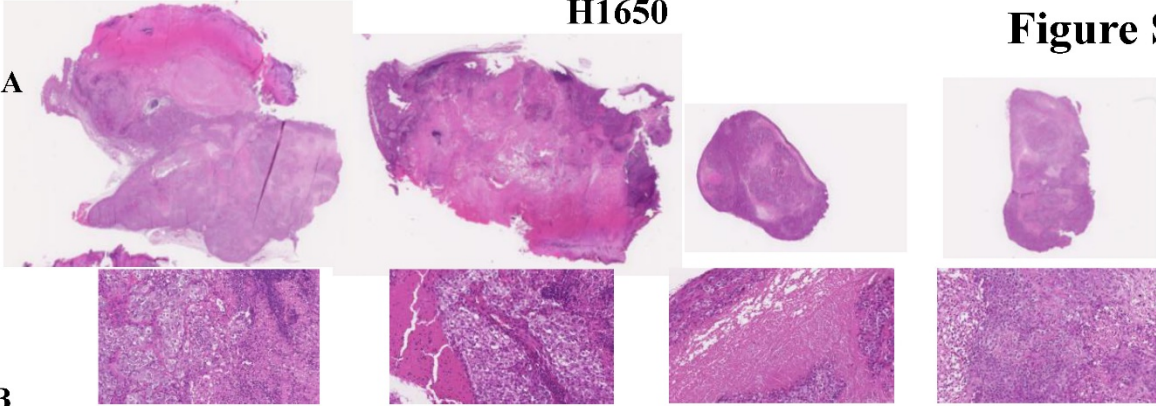


Figure S7

H1650

Figure S8

A



B

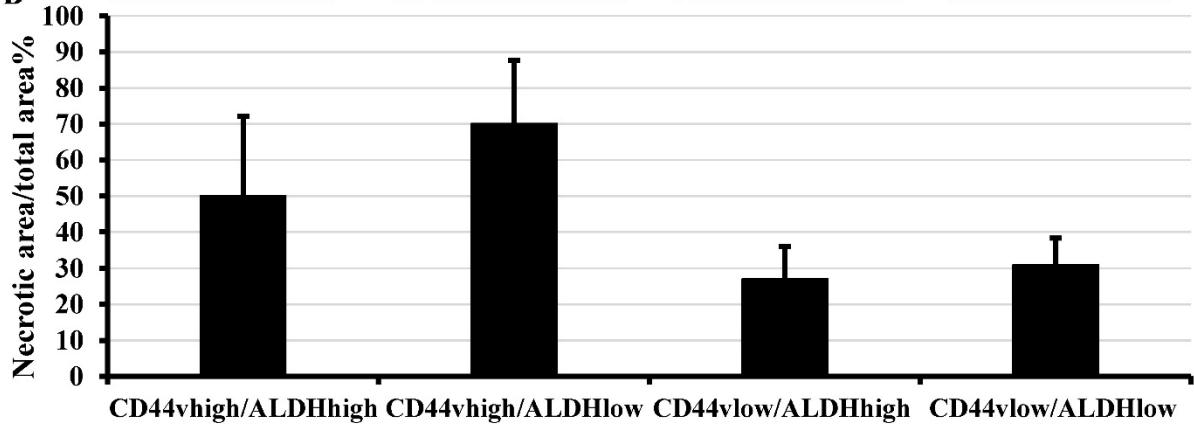
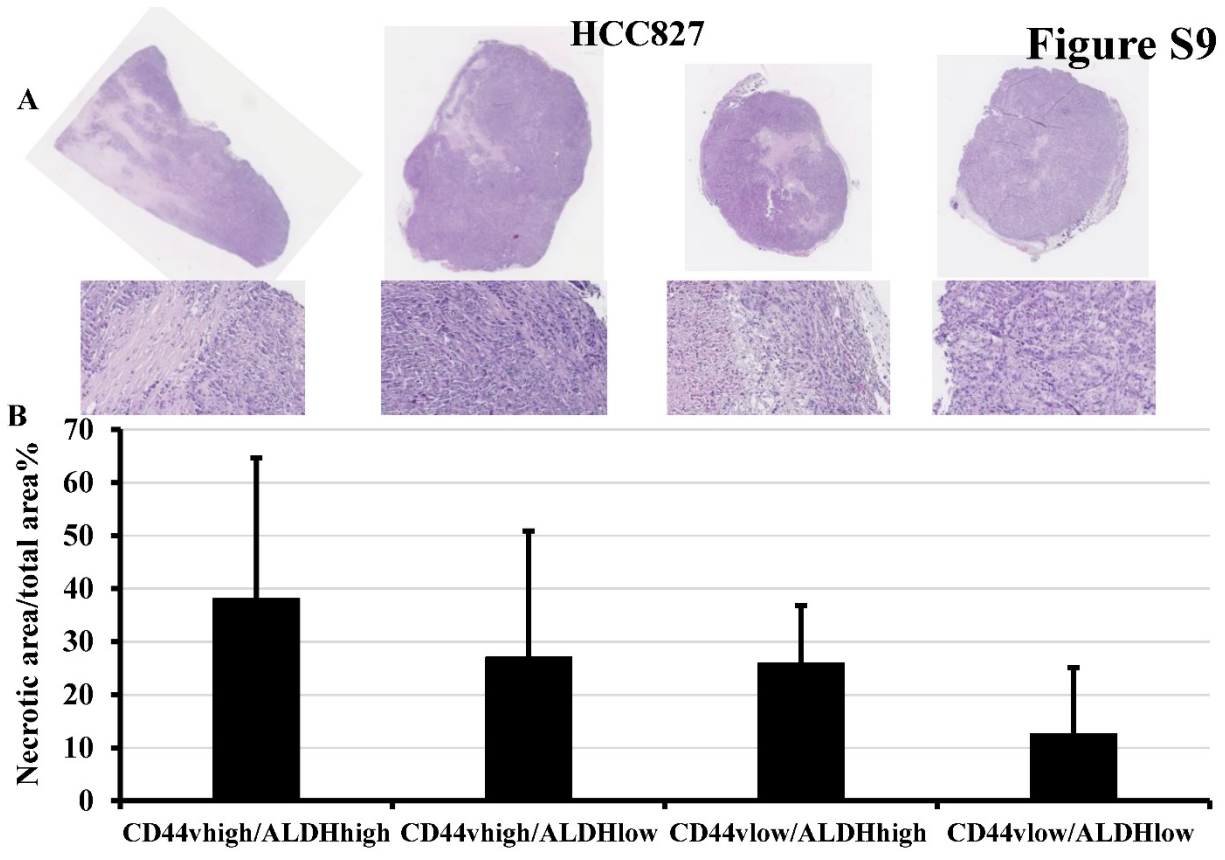


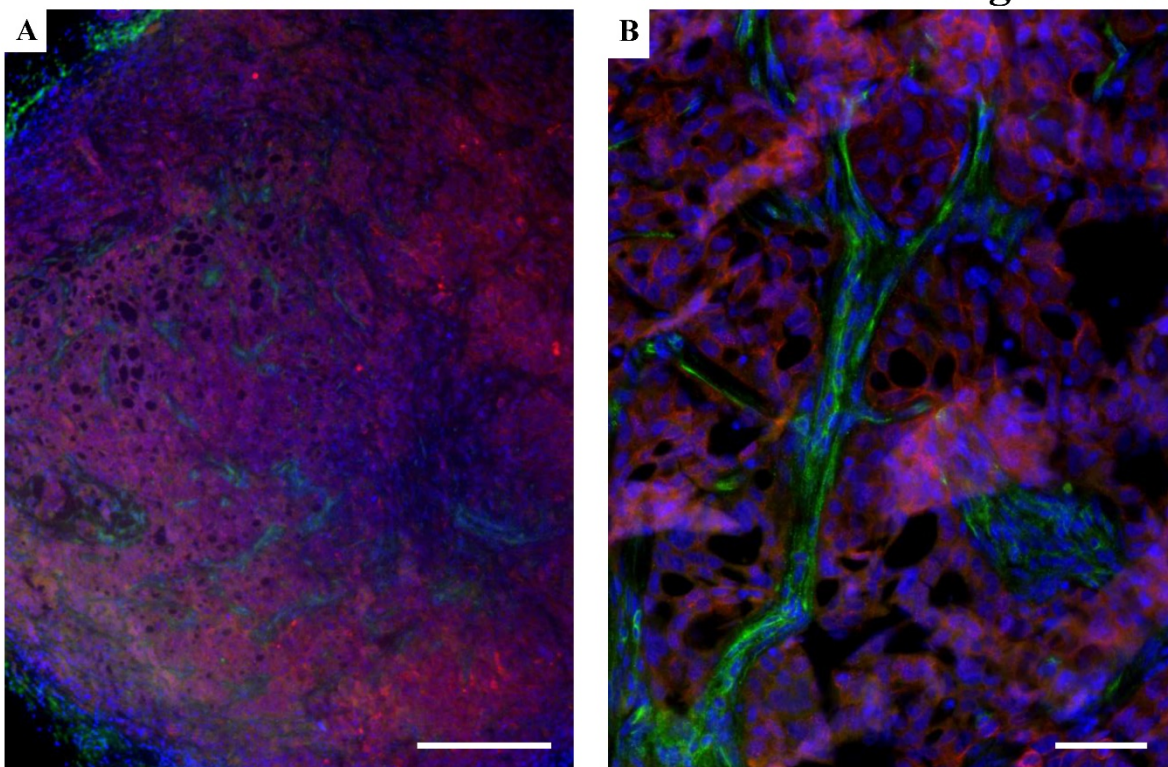
Figure S9

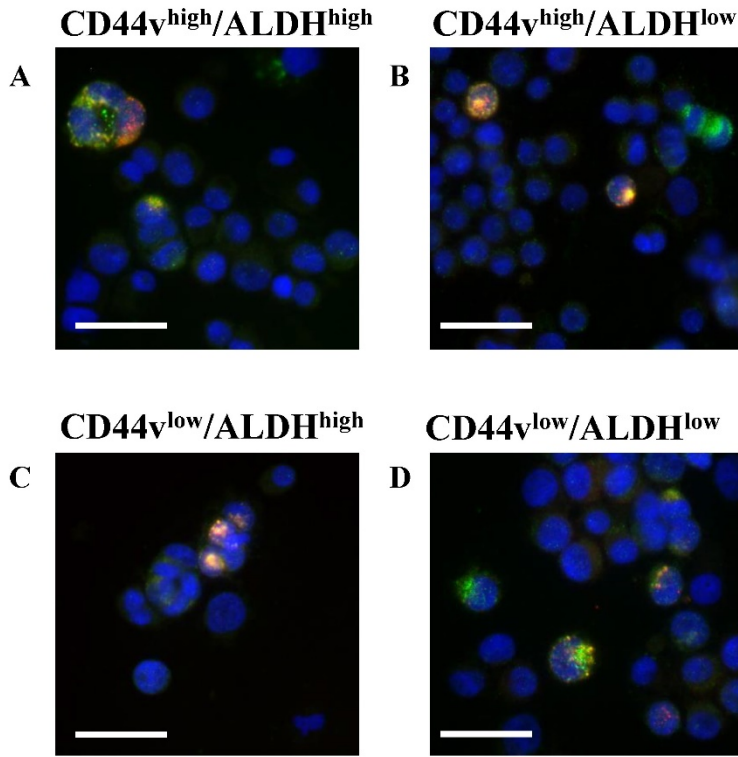


E-cadherin/CD34/DAPI

HCC827

Figure S10





EGFR/pEGFR/DAPI

Figure S11

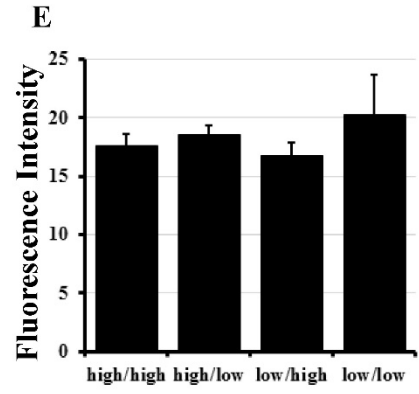
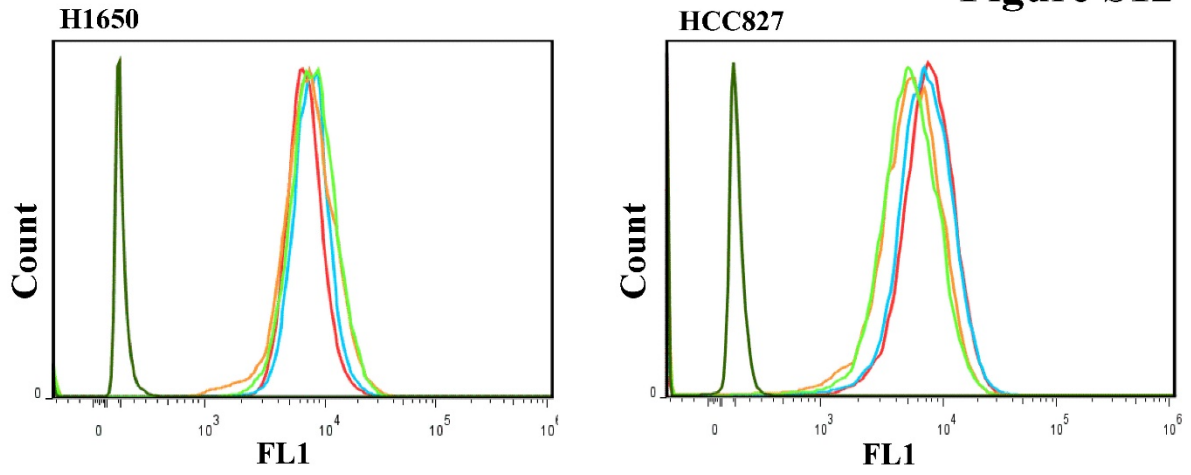


Figure S12



	Sample Name
	Unstained control
	CD44 ^{v^{high}} /ALDH ^{high}
	CD44 ^{v^{low}} /ALDH ^{high}
	CD44 ^{v^{low}} /ALDH ^{low}
	CD44 ^{v^{high}} /ALDH ^{low}